

# Morphed Face Detection Based on Deep Color Residual Noise

Sushma Venkatesh<sup>†</sup>, Raghavendra Ramachandra<sup>†</sup>, Kiran Raja<sup>†</sup>,  
Luuk Spreeuwiers<sup>‡</sup>, Raymond Veldhuis<sup>‡</sup>, Christoph Busch<sup>†</sup>

<sup>†</sup>Norwegian Biometrics Laboratory, NTNU - Gjøvik, Norway

<sup>‡</sup>University of Twente, Enschede, Netherlands.

{sushma.venkatesh; raghavendra.ramachandra;kiran.raja;christoph.busch}@ntnu.no  
{l.j.spreeuwiers;r.n.j.veldhuis@utwente.nl}

**Abstract**—Secure access control applications like border control rely on the face based verification system by considering its reliability, usability and accuracy in-person verification. However, face recognition systems are vulnerable to morphed face attacks, in which, the morphing process combines two different facial images into a single facial image. The features extracted from the morphed face image will match to those extracted from probe images of both faces. Thus, it is essential to reliably detect the morphed face image attacks on the face recognition systems. In this work, we propose a novel approach to detect morphed face images using residual color noise. The proposed method is designed to capture the noise patterns that are a result of the morphing process. Thus, the proposed method performs first denoising using Deep Convolutional Neural Network (CNN) independently on the Hue Saturation Value (HSV) color space, and then computes the residual noise. The extracted residual noise is further processed using Pyramid Local Binary Patterns (P-LBP), which is further classified using the Spectral Regression Kernel Discriminant Analysis (SRKDA). Extensive experiments are carried out on three different morphed face image datasets. The Morphed Attack Detection (MAD) performance of the proposed method is benchmarked with 13 different state-of-the-art techniques using the ISO IEC 30107-3 evaluation metrics. Based on the obtained quantitative results, the proposed method has indicated the best performance.

**Index Terms**—Biometrics, face recognition, Morphing attacks, Morphing Attack Detection

## I. INTRODUCTION

Biometric systems employing face, fingerprint or iris recognition are widely deployed to verify the unique identity of an individual in various access control applications. Face Recognition Systems (FRS) are predominantly deployed to verify and establish an identity due to the ease of capture process in a non-invasive manner and at a distance. At the same time, face images are also used in passport based verification both for border crossing and International Civil Aviation Organization (ICAO) based identity verification amongst others. Recently well-used identity check in the airport involves an individual presenting his electronic Machine Readable Travel Document (eMRTD) to verify identity either via Automated Border Control (ABC) gates or to an immigration officer.

While the identity can be verified against a presented image on the passport, many countries issue such documents based



Fig. 1: Example of the morphed face image

on the printed face photo provided by the applicant. Malicious actors can therefore use such an opportunity to provide a tampered face image. One critical case of a tampered face image defeating the FRS is reported as morphed face image, which can successfully verify against multiple individuals. Morphing is an image processing technique used to combine face images of two different individuals, to obtain a single face image. Morphing poses a great threat for the identity check in passport control, as an authentic eMRTD, containing a morphed image, can be used by two different individuals. This applies to the visual inspection process by a border guard, but also to automated processing, when the verification is conducted with the commercial-off-the-shelf (COTS) FRS [3]. The challenge becomes critical, when malicious actors morph the face image against the non-blacklisted subject. This poses a potential threat to security of the border control and thereby it is essential to identify such morphed face images. Motivated by the gravity of the problem, recent research works are focused on detecting morphed images to identify a possible attack on the face recognition system. As indicated in [12], there exists two different techniques for Morphing Attack Detection (MAD): (i) No reference morphing attack detection technique (ii) Differential morphing attack detection techniques. In the former morphing detection technique, an image is analyzed individually without any reference and then classified as a bona fide image or morphed image. In the latter, an image is analyzed based on the stored reference image by using a obtained reference image, for instance using a live captured image (from Automatic Border Control (ABC) gate) compared against stored reference eMRTD image. In

such a scenario, the eMRTD image is classified as bona fide, if the MAD-features of live captured image from the ABC-gate correspond to the extracted MAD-features of the eMRTD image. Further, the no reference morphing attack detection can be of two types depending upon the type of processing of the image data such as [7]: (a) print-scan attack detection in which the digital photo captured in the photo booth (or studio) is then printed and handed over to the passport issuance center, where it is again digitised using a scanning device and subsequently stored in the eMRTD. (b) Digital attack detection, where the captured face digitally can be used directly to detect the morphing attacks. since the digital passport photos are used in many countries to renew the passport applications [7]. In this work, we focus on detecting digital face morphed attacks by considering its wide applicability in real-life applications and also it is easy to generate these attacks [7].

The digital morphed face detection is widely addressed in the literature that has resulted in several techniques that can be broadly divided into three types: (a) Texture based (b) image quality based (c) deep learning based approaches. Early works are based on hand-crafted texture-based techniques that are expected to capture the variation in micro textures during the process of morphing that facilitates morph detection. To this extent, several algorithms-based on texture features such as Binary Statistical Image Features (BSIF), Local Phase Quantization (LPQ) [7] and Local Binary Pattern (LBP) [7], [15] and its variants are introduced to detect the digital version of morphed faces. Among these texture-based techniques, the use of LBP and BSIF has indicated consistent morphed face detection performance. The image quality-based methods are designed to quantify the variation in the compression artefacts and morphing noise introduced during the process of morph generation. Several approaches are presented that includes analysis of Benford features distribution that varies after the jpeg compression [6]. spectral analysis of PRNU [2] and StirTrace [4]. Recent approaches are based on using the deep learning approaches, especially on using the pre-trained CNN architecture like AlexNet, VGG, ResNet, GoogleNet and InceptionV3 [9], [13]. Based on the several experiments reported in the literature, the deep learning-based approaches and the image degradation approaches shows the improved performance over texture-based approaches.

In this work, we present a new approach for no-reference morphing face attack detection by analysing the residual noise that may be attributed due to the process of face morphing. Specifically, we compute the residual noise using a Deep-CNN based denoising network on each of the color channels of the given face image. On the obtained residual noise of each channel, we further extract the textural features using the Pyramidal Local Binary Pattern (P-LBP) to better quantify the noise patterns. Finally, we learn a spectrally regressed kernel discriminant (SRKD) to discriminate between the bona fide and morphed image. To validate the intuition of our proposed approach, we employ three different large scale datasets compromised of bona fide and morphed images. Through empirical evaluation on these three large scale datasets, we demonstrate

a superior Morphing Attack Detection (MAD) performance and further compare it against the detection performance of hand-crafted and deep-learning features. The key contributions of this work includes: (1) Novel method for morphed face detection based on the color residual noise computed based on D-CNN denoising technique. (2) Extensive experiments are carried out on three different face morphing datasets and the performance of the proposed method is benchmark with 13 different state-of-the-art techniques.

The rest of the paper is organized in the following order: Section II presents our proposed method. Section III describes the experiments and results obtained. Finally, Section IV draws the conclusion.

## II. PROPOSED METHOD

Figure 2 shows the functional block diagram of the proposed method for the proposed face morphing detection. The face morphing process combines two face images using mathematical operations to obtain the morphed face image. This results in the morphed image that adulterates the noisy components due to pixel discontinuities. Thus, we assert that computing these residual noises that are expected to be in high magnitude in the morphed face images when compared to that of the bona fide face images. Such irregularities can help in revealing the morphed manipulation. The proposed method is structured to compute the residual noise from the individual color spaces. Given the color (RGB) face image  $I_{RGB}$ , the first step is to decompose the image into HSV color space that can better capture the distinct characteristics of the bona fide and morphed images. For example, the morphed images may have different characteristics of edges, textures, shade and color smoothness. These characteristics can be best described by decoupling the intensity from the chroma component using HSV color space. Let the HSV color image can be represented as  $I_{HSV}$ .

In the next step, the image denoising is carried out on individual color channels. To this extent, we propose to employ, the Denoise Deep Convolutional Neural Network (De-DCNN) denoising method from [16] by considering its denoising performance. In this work, we use the pre-trained De-DCNN that is trained using natural images with a large variety of noise [16]. We then carry out the denoising of individual color channels to get corresponding denoised images:  $I'_H, I'_S, I'_V$ . In the next step, we compute the residual noise independently on three channels as:  $RN_H = I_H - I'_H$ ,  $RN_S = I_S - I'_S$ ,  $RN_V = I_V - I'_V$ . Figure 3 illustrates the residual noise computed from the HSV color space that clearly indicates the distinction between bona fide and morphed image.

In the next step, we further process the residual noise images using Pyramid-Local Binary Component (P-LBP) features to quantify the residual noise effectively. We are motivated to employ this approach by considering its efficiency in modeling the residual noise as indicated in [17]. In this work, we use the Laplacian Pyramid with three level decomposition independently on residual noise image on which the LBP is computed. Given the

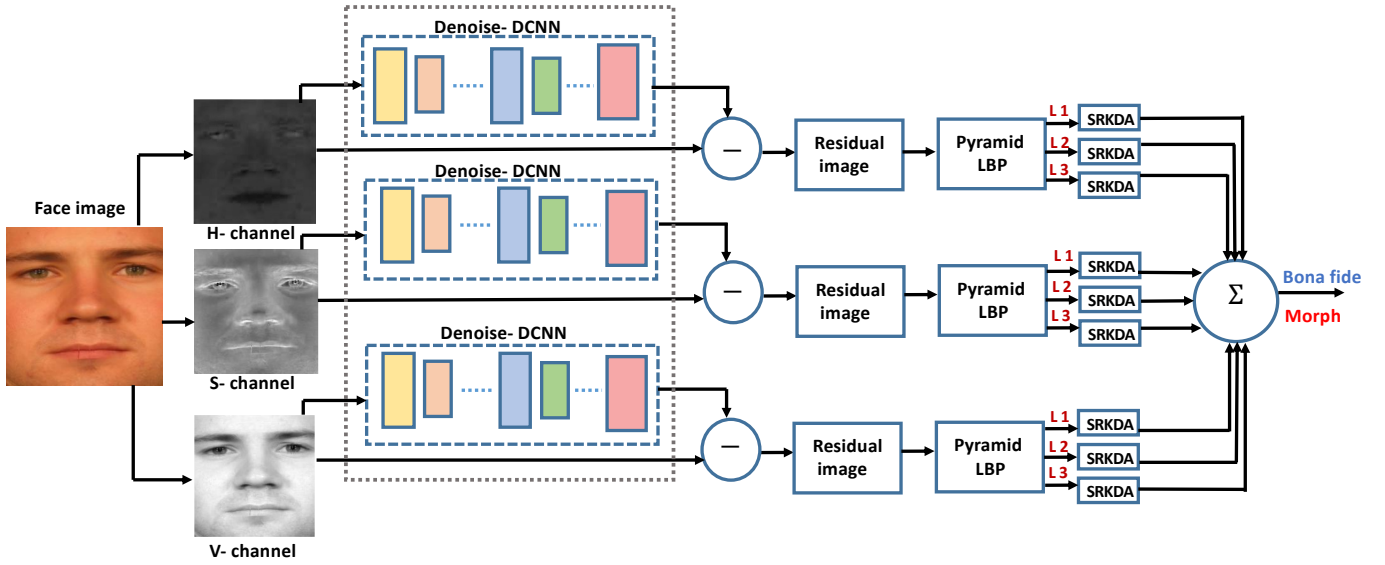


Fig. 2: Block diagram of the proposed method

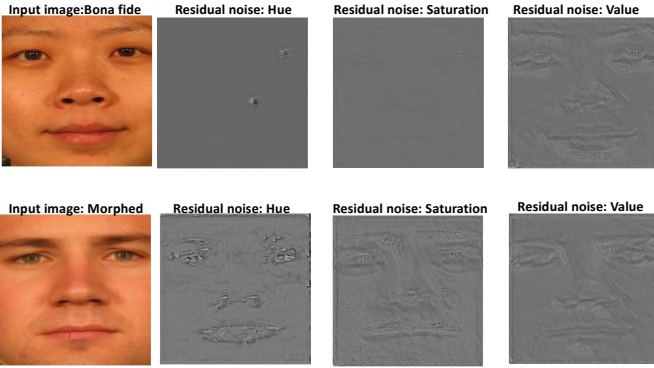


Fig. 3: Illustration of the residual noise image computed using proposed method on (a) Bona fide image (b) Morphed image

residual image, the proposed method provides three sets of features computed using LBP corresponding to three level Laplacian pyramid. Thus, in total there are 9 different P-LBP features computed from 3 different residual noise images as:  $RN_H^{L1}, RN_H^{L2}, RN_H^{L3}, RN_S^{L1}, RN_S^{L2}, RN_S^{L3}, RN_V^{L1}, RN_V^{L2}, RN_V^{L3}$ . Finally, we train the morph detector based on Spectral Regression Kernel Discriminant Analysis [1] independently on nine different features using a training set. Given the test image, we compute the Morph Attack Detection (MAD) score corresponding to 9 different features as:  $MD_{f1}, MD_{f2}, MD_{f3}, MD_{f4}, MD_{f5}, MD_{f6}, MD_{f7}, MD_{f8}, MD_{f9}$ . Final decision is computed by combining the MAD scores using a sum rule as:  $\sum_{i=1}^9 MD_{fi}$ .

### III. EXPERIMENTS AND RESULTS

In this section, we present the quantitative results of the proposed method together with 13 different State-Of-The-Art (SOTA) techniques for the morphed face image detection. Experimental results are presented using the ISO30107-3 [5]

metrics such as Bona fide Presentation Classification Error Rate (BPCER(%)) and Attack Presentation Classification Error Rate (APCER (%)) along with D-EER(%). BPCER defines the proportion of bona fide presentations incorrectly classified as attack images and APCER defines attack images incorrectly classified as the bona fide images [5].

Extensive experiments are presented on three different datasets namely: **Dataset-1**: This dataset is constructed using 179 unique subjects that are divided into two disjoint independent sets namely training (89 subjects) and testing (90 subjects). These subjects are selected using both publicly available and private face datasets. The morphing process is carried out using the open source tool mentioned in [8] that has resulted in a training set with 709 bona fide and 1255 morphed images and testing set with 918 bona fide and 1354 morphed images. Figure 4 (a) shows the example of the bona fide and morphed images. **Dataset-2**: This dataset is constructed using the FRGC dataset in which 568 data subjects are used to generate morphed images using an automatic method based on facial landmark and triangulation as described in [15]. This dataset has 300 bona fide and 3041 morphed images corresponding to 300 data subjects used as the training set. While the testing set is generated using 268 data subjects that correspond to 268 bona fide and 2739 morphed images. Figure 4 (b) illustrates the example image from this dataset. **Dataset-3**: This dataset is comprised of 100 data subjects selected from putDB dataset which is publicly available. The training dataset is comprised of 50 data subjects that are used to generate 50 bona fide and 254 morphed samples. The testing dataset is comprised of 50 data subjects that are used to generate 50 bona fide and 244 morphed images. The morphing process is based on facial landmark and triangulation as described in [15]. Figure 4 (c) shows the example of the bona fide and morphed images.

In this work, we have evaluated 6 deep learning based SOTA

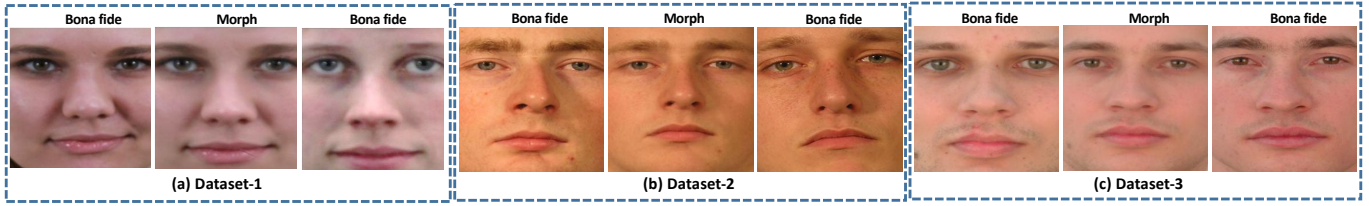


Fig. 4: Illustration of the example images from (a) Dataset-1 (b) Dataset-2 (c) Dataset-3

TABLE I: Quantitative performance of the MAD algorithms on Experiment-1 (individual dataset)

Algorithms	Database-1			Database-2			Database-3		
	D-EER(%)	BPCER@ APCER		D-EER(%)	BPCER@ APCER		D-EER(%)	BPCER@ APCER	
		=5%	=10%		=5%	=10%		=5%	=10%
AlexNet-SVM [10]	5.50	3.5	2.33	7.08	8.95	4.85	11	22	12
GoogleNet-SVM [10]	9.63	13.66	8.83	11.95	22.38	14.55	42.23	100	77.23
InceptionV3-SVM [10]	11.66	18.83	12.33	8.21	11.94	8.20	11.94	26	16
ResNet101-SVM [10]	5.51	6.16	4	6.48	6.10	4.74	13.76	32	22
VGG16-SVM [10] [9]	13.31	25	16.83	14.50	28.35	18.28	21.86	100	36
VGG19-SVM [10] [14]	12.49	22.66	15	12.32	22.38	14.17	24.50	52	40
BSIF-SVM [11]	26.70	53	42	12.67	25.74	14.55	20.45	44	32
Steerable pyramid-SVM [10]	26.19	65.50	50	37.97	82.08	71.64	34.00	82	70
HOG-SVM [11]	10.37	19.83	10.50	12.30	23.50	14.92	11.91	26	10
Image Gradient-SVM [7]	17.34	38	26.50	25.24	51.86	39.92	31.98	72	60
LBP-SVM [7]	18.67	39.16	28.16	9.31	14.55	8.20	22.06	62	38
PRNU [2]	26.51	57.16	44.67	39.89	78.35	70.15	35.62	74	58
LPQ-SVM [7]	17.30	43.66	28.66	13.43	26.11	16.41	20.24	56	38
<b>Proposed Method</b>	<b>3.83</b>	<b>3</b>	<b>1.5</b>	<b>4.85</b>	<b>4.85</b>	<b>3.35</b>	<b>9.71</b>	<b>14</b>	<b>8</b>

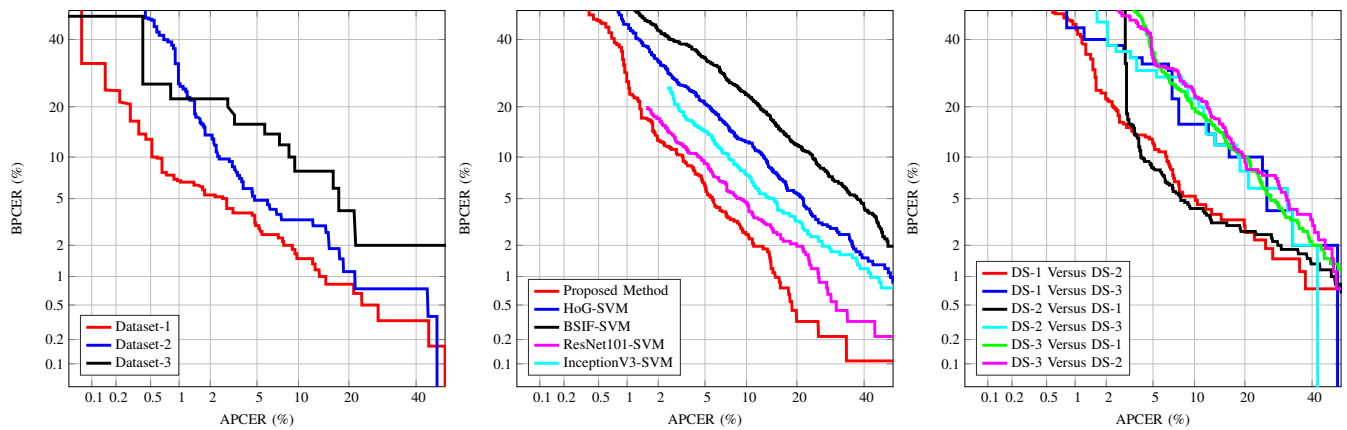


Fig. 5: DET Curves (a) performance of the proposed method on three different datasets in Experiment-1 (b) performance of the top five MAD algorithms including the proposed method on Experiment-2 (c) performance of the proposed method in Experiment-3 (cross dataset)

and 7 non-deep learning based techniques. In case of deep learning technique, we have used the pre-trained network and compute the corresponding features that are further classified using linear Support Vector Machines (SVM). To this extent, we have considered pre-trained CNN such as AlexNet [10], GoogleNet [10], Inception V3 [10], ResNet101 [10], VGG16 [10] and VGG19 [10]. In case of non-deep learning techniques, texture-based techniques such as; LBP [7], LPQ [7], BSIF [11], Steerable Pyramids [10] together with image distortion based features such as Image gradients [7], HoG [11] and PRNU [2] are used together with linear SVM (except for PRNU) to compute the detection performance. To effectively evaluate the performance of the Morph Attack Detection (MAD) schemes, we perform three different experiments such as **Experiment-1:-** is designed to evaluate the performance of the MAD schemes when training and testing are done on the same dataset. **Experiment-2:-** is designed to evaluate the MAD schemes on the merged dataset in which all three datasets are merged into one dataset. This experiment provides an insight into the MAD performance when the dataset is increased with a number of samples. **Experiment-3:-** is designed to perform the cross-dataset comparison in which one of the datasets is used for training and another dataset is used for testing. This experiment will highlight insights on MAD techniques that tested on the unknown dataset.

Table I shows the quantitative performance of the proposed method, along with 13 different SOTA techniques on Experiment-1. It is interesting to note that (1) the MAD performance of the deep learning features shows the improved performance over non-deep learning methods on all three datasets. (2) Among three different the performance of the all MAD techniques indicate the degraded performance that can be attributed to the characteristics of the dataset. (3) The ReseNet101 and Inception V3 based features indicate better performance over other DCNN features on all three datasets. (4) Among the non-deep features, LBP and HoG schemes indicate better performance over other non-deep features on all three datasets. (5) The proposed method has indicated the best performance when compared to that of the 13 different SOTA techniques on all three different datasets. Figure 5 (a) shows the DET curves indicating the performance of the proposed method on all three datasets evaluated in this work.

Table II indicates the quantitative performance of the proposed method on the Experiment-2 in which all three datasets are merged. Based on the obtained results, the deep features indicate better performance over non-deep techniques. Further, the proposed method has indicated the best performance with D-EER = 5.34% with BPCER = 6.31% @APCER = 5% and BPCER = 2.50% @APCER = 10%. These obtained results further justify the robustness of the proposed method to the increased number of samples with different image characteristics. Figure 5 (b) shows the DET curves indicating the performance corresponding to the top five best performing techniques including the proposed method.

Table III indicates the quantitative performance of the proposed method on the Experiment-3 (cross-dataset evaluation).

TABLE II: Quantitative performance of the MAD algorithms on Experiment-2 (merged dataset)

Algorithms	D-EER(%)	BPCER@ APCER	
		=5%	=10%
AlexNet-SVM [10]	9.70	17.32	9.36
GoogleNet-SVM [10]	10.87	21.35	11.98
InceptionV3-SVM [10]	8.69	14.59	7.51
ResNet101-SVM [10]	7.77	9.04	4.68
VGG16-SVM [10]	12.83	25.49	15.03
VGG19-SVM [10]	12.19	24.50	15.03
BSIF-SVM [11]	15.58	33.98	23.09
Steerable Pyramid-SVM [10]	36.78	77.88	68.08
HOG-SVM [11]	11.32	20.69	12.52
Image Gradient-SVM [7]	38.41	79.84	68.84
LBP-SVM [7]	36.58	73.42	63.98
PRNU [2]	36.88	76.84	65.35
LPQ-SVM [7]	15.03	30.28	19.82
<b>Proposed Method</b>	<b>5.34</b>	<b>6.31</b>	<b>2.50</b>

TABLE III: Quantitative performance of the MAD algorithms on Experiment-3 (cross Dataset)

Training Dataset	Test Dataset	Algorithms	D-EER(%)	BPCER@ APCER	
				=5%	=10%
Database-1	Database-2	Alexnet-SVM [10]	50	100	100
		Resnet101-SVM [10]	50	100	100
		HoG-SVM [11]	17.97	38.43	28.35
		<b>Proposed method</b>	<b>7.12</b>	<b>12.31</b>	<b>5.22</b>
Database-1	Database-3	Alexnet-SVM [10]	19.63	32	24
		Resnet101-SVM [10]	13.96	100	18
		HoG-SVM [11]	20.24	50	30
		<b>Proposed method</b>	<b>13.76</b>	<b>32</b>	<b>16</b>
Database-2	Database-1	Alexnet-SVM [10]	8.14	11.66	7.33
		Resnet101-SVM [10]	9.82	16.33	9.66
		HoG-SVM [11]	6.81	9	4.83
		<b>Proposed method</b>	<b>6.49</b>	<b>8.50</b>	<b>4.16</b>
Database-2	Database-3	Alexnet-SVM [10]	19.83	38	34
		Resnet101-SVM [10]	13.76	26	16
		HoG-SVM [11]	12.35	34	20
		<b>Proposed method</b>	<b>13.76</b>	<b>30</b>	<b>22</b>
Database-3	Database-1	Alexnet-SVM [10]	50	100	100
		Resnet101-SVM [10]	14.68	100	18.83
		HoG-SVM [11]	14.52	32	19.16
		<b>Proposed method</b>	<b>14.40</b>	<b>36.16</b>	<b>19.50</b>
Database-3	Database-2	Alexnet-SVM [10]	50	100	100
		Resnet101-SVM [10]	17.27	100	100
		HoG-SVM [11]	24.28	58.20	42.53
		<b>Proposed method</b>	<b>15.31</b>	<b>33.95</b>	<b>23.50</b>

For simplicity, we have presented the results only for the top four best performing MAD techniques based on Experiment-1 and Experiment-2. Since we have three different datasets, we get six different cases in which one dataset is enrolled and the remaining two datasets are probed. Based on the obtained results, the proposed method shows improved performance when compared with the SOTA methods. However, when dataset-3 is used as the probe, the performance of the proposed method is comparable with the SOTA methods. Figure 5 (c) shows the DET curves of the proposed method on all six different cases of cross dataset comparison. For simplicity, we

have indicated DET curves for selected techniques, however, detailed quantitative results are presented in Table I, Table II & Table III.

Thus, based on the extensive experiments carried out on three different datasets, the proposed method has indicated the best MAD performance when compared with 13 different SOTA techniques. Quantitative results obtained on three different experiments shows the best performance of the proposed method, which justifies the applicability of the residual noise computed based on the deep denoising technique for the robust morphed face detection.

#### IV. CONCLUSION

In this work, we propose a novel method based on denoising to identify the presence of a morph attack. Existence of residual noise that is obtained after getting the difference of the face image with its denoised version indicates the presence of morphing. Face image in HSV color space is denoised to obtain the difference image that is obtained by subtracting the given image with its denoised version in HSV color space. Difference obtained after subtraction is the residual noise on which pyramid LBP is applied to get the spatial features with three level decomposition. Further the spatial features are classified using SRKDA classifier to reliably identify the given image as bona fide or morphed.

Extensive experiments are carried out on three different morphed face databases (digital version). We present an evaluation on 13 different algorithms based on deep learning and non-deep learning features. Among six different deep features and seven different non-deep features our proposed method based on denoising outperforms the existing techniques. Performance of the proposed method on dataset-1 gives a D-EER of 3.83% with BPCER = 1.5% at APCER = 10% and BPCER = 3% at APCER = 5%. dataset-2 gives a D-EER of 4.85% with BPCER = 3.35% at APCER = 10% and BPCER = 4.85% at APCER = 5%. Finally dataset-3 presents a D-EER of 9.71% at BPCER = 8% at APCER = 10% and BPCER = 14% at APCER = 5%. Quantitative results obtained on all three datasets indicates the consistent performance that shows the robustness and reliability of the proposed method.

#### REFERENCES

- [1] D. Cai, X. He, and J. Han. Speed up kernel discriminant analysis. *The VLDB Journal The International Journal on Very Large Data Bases*, 20(1):21–33, 2011.
- [2] L. Debiasi, U. Scherhag, C. Rathgeb, A. Uhl, and C. Busch. Prnu-based detection of morphed face images. In *2018 International Workshop on Biometrics and Forensics (IWBF)*, pages 1–7, 2018.
- [3] M. Ferrara, A. Franco, and D. Maltoni. Face demorphing. *IEEE Transactions on Information Forensics and Security*, 13(4):1008–1017, 2018.
- [4] M. Hildebrandt, T. Neubert, A. Makrushin, and J. Dittmann. Benchmarking face morphing forgery detection: Application of stirtrace for impact simulation of different processing steps. In *International Workshop on Biometrics and Forensics (IWBF 2017)*, pages 1–6, 2017.
- [5] ISO/IEC JTC1 SC37 Biometrics. *ISO/IEC 30107-3. Information Technology - Biometric presentation attack detection - Part 3: Testing and Reporting*. International Organization for Standardization, 2017.
- [6] A. Makrushin, T. Neubert, and J. Dittmann. Automatic generation and detection of visually faultless facial morphs. In *Proceedings of the 12th International Joint Conference on Computer Vision, Imaging and Computer Graphics Theory and Applications - Volume 6: VISAPP, (VISIGRAPP 2017)*, pages 39–50. INSTICC, SciTePress, 2017.
- [7] R. Raghavendra, K. B. Raja, and C. Busch. Detecting Morphed Face Images. In *8th IEEE International Conference on Biometrics: Theory, Applications, and Systems (BTAS)*, pages 1–8, 2016.
- [8] R. Raghavendra, K. B. Raja, S. Venkatesh, and C. Busch. Face morphing versus face averaging: Vulnerability and detection. In *IEEE International Joint Conference on Biometrics (IJCB)*, pages 555–563, 2017.
- [9] R. Raghavendra, K. B. Raja, S. Venkatesh, and C. Busch. Transferable deep-cnn features for detecting digital and print-scanned morphed face images. In *Proc. IEEE Conf. Computer Vision Pattern Recognition Workshops (CVPRW)*, pages 1822–1830, 2017.
- [10] R. Raghavendra, S. Venkatesh, K. Raja, and C. Busch. Detecting face morphing attacks with collaborative representation of steerable features. In *IAPR International Conference on Computer Vision & Image Processing (CVIP-2018)*, pages 1–7, 2018.
- [11] U. Scherhag, R. Raghavendra, K. Raja, M. Gomez-Barrero, C. Rathgeb, and C. Busch. On the vulnerability of face recognition systems towards morphed face attack. In *International Workshop on Biometrics and Forensics (IWBF 2017)*, pages 1–6, 2017.
- [12] U. Scherhag, C. Rathgeb, J. Merkle, R. Breithaupt, and C. Busch. Face recognition systems under morphing attacks: A survey. *IEEE Access*, 7:23012–23026, 2019.
- [13] C. Seibold, W. Samek, A. Hilsmann, and P. Eisert. Detection of face morphing attacks by deep learning. In *International Workshop on Digital Watermarking*, pages 107–120, 2017.
- [14] C. Seibold, W. Samek, A. Hilsmann, and P. Eisert. Detection of face morphing attacks by deep learning. In C. Kraetzer, Y.-Q. Shi, J. Dittmann, and H. J. Kim, editors, *Digital Forensics and Watermarking*, pages 107–120. Springer International Publishing, 2017.
- [15] L. Spreeuwers, M. Schils, and R. Veldhuis. Towards robust evaluation of face morphing detection. In *2018 26th European Signal Processing Conference (EUSIPCO)*, pages 1027–1031, Sep. 2018.
- [16] K. Zhang, W. Zuo, Y. Chen, D. Meng, and L. Zhang. Beyond a gaussian denoiser: Residual learning of deep CNN for image denoising. *CoRR*, abs/1608.03981, 2016.
- [17] Y. Zhang, S. Fang, Y. Xie, and T. Xu. Fake fingerprint detection based on wavelet analysis and local binary pattern. In *Biometric Recognition*, pages 191–198, 2014.